LIGANDS BINDING [Fe_2–S_2] CLUSTER PROTEINS: DFT APPROACH FOR DRUG-LIKENESS ASSESSMENT

Maria PETRESCU[1,2], Misu MOSCOVICI[2], Amalia STEFANIU[3]

Different small molecules as mono- or bidentate ligands, synthesized outside their protein environments, are used as models to better understand the biological properties and functions of Fe-S clusters, gaining insights on their structural diversity and complexity with important biological implications. In this work, investigations aiming to assess molecular properties and structural descriptors on several non-hydrogenase [Fe2-S_2] small-molecule models reported in the literature data since 2010 and characterized by their redox potential, are carried out using B3LYP/DFT functional. Emphasis is placed on drug-like properties and quantum chemical reactivity parameters of several S and/or N ligands to exploit their potential to bind iron-sulfur cluster proteins and to understand the redox active behaviour of such bioinorganic species. By using such an approach, we obtained useful data on several ligands coordinating to an Fe-S cluster. The predicted properties can be further used to highlight the correlation between applications based on the structure–function relationship of Fe-S clusters and the nature of their ligands.

Keywords: Fe-S clusters; ligands; QSAR properties, quantum predictions.

1. Introduction

Fe-S clusters are involved in broad processes essential for the cellular function; due to their different roles, Fe-S clusters can be used in the development of new therapeutic strategies to treat a wide range of human diseases such as type II diabetes, breast cancer, skin cancer, kidney cancer, tuberculosis, malaria and other bacterial or viral infections. In most cases, inhibitors are designed for a receptor protein containing an Fe-S cluster, correlated with a disease phenotype [1]. Three main strategies have been identified to inhibit Fe-S protein activity: the ligand binds to the protein in the vicinity of its Fe-S cluster; the ligand binds directly to the Fe-S cluster through open coordination or through the active site of the substrate, or the ligand causes degradation of the [Fe_4S_4] cluster to [Fe_3S_4] cluster or produces complete degradation of the cluster [2]. Most of the strategies need advanced research to develop safe and effective therapies. Research directions requiring a more in-depth approach include studying virulence mechanisms for each target, designing more inhibitors with drug potential, and testing the specificity of these molecules in mammals.

[1] PhD student, Faculty of Chemical Engineering and Biotechnologies (FCEB), National University of Science and Technology POLITEHNICA of Bucharest (NUSTPB), Romania, e-mail: maria.m.petrescu@gmail.com
[2] PhD. Eng., National Institute for Chemical and Pharmaceutical Research and Development (ICCF) Bucharest, Romania, e-mail: misu_moscovici@hotmail.com
[3] PhD. Eng., National Institute for Chemical and Pharmaceutical Research and Development (ICCF) Bucharest, Romania, e-mail: astefaniu@gmail.com

Cosconati et al [3] applied a virtual ligand screening against a validated target of antibiotic-resistant *Mycobacterium tuberculosis*, Fe-S adenosine 5' phosphosulfate reductase, and 5 first non-phosphate leading compounds inhibitors at the binding site were identified from the Development Therapeutics Program (DTP) of The National Cancer Institute (NCI), USA (http://dtp.nci.nih.gov/). Their structures, autodock binding energies, and activities were presented. Mike et al. [4] identified, by experimental high-throughput screening aiming at hem activation biosynthesis, a molecule named *`882* and one of its derivatives, more active in an in vivo model, which by accumulation, reaches toxic concentrations against a *Staphylococcus aureus* methicillin-resistant strain (MRSA), thus explaining its bacteriostatic activity. Later, its inhibitory activity against some Fe-S proteins maturation, probably hindering the cluster integration in apoproteins, was highlighted by Choby et al. [5]; Dutter et al. [6] synthesized `882 derivatives, who's inhibitory (toxic) activity of those compounds against the microorganism was decoupled from the hem biosynthesis activation.

Small-molecule [Fe_2–S_2] clusters (Fig. 1) are generally obtained by the reaction of ferric or ferrous tetrathiolate complexes with elemental sulfur or by the reaction of ferric chloride, thiolate, hydrosulfide, and methoxide [7].

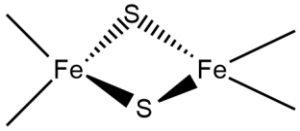

Fig. 1. [Fe_2–S_2] clusters structure

Another pathway to generate [Fe_2–S_2] clusters is by using alkylthiolate ligands in reaction with mononitrosyl iron complex, following the addition of methyl 3-mercaptopropionate [8]. Cysteine, cysteinate, and cysteine analogues are involved in the regeneration of [Fe_2–S_2] clusters, which are damaged by nitric oxide, by destabilization of mononitrosyl iron complex [8,9]. Bacterial oxygenases and ferredoxins contain [Fe_2–S_2] iron-sulfur cluster linked to protein via two histidine and two cysteine residues, known as catalytic Rieske centres [10], involved in redox reactions. The first synthetic analogue of Rieske proteins containing an asymmetric synthetic [Fe_2–S_2] cluster was reported by Ballmann J. et al. [11] in 2008.

In this work, we aimed to complete the previous works on design, synthesis and experimental redox potential of several ligands, gathered by Boncella A.E. et al. [2] by in silico studies referring to predictive calculations of the properties of possible ligands for Fe-S proteins capable of binding in the cluster' active site and producing redox reactions leading to the degradation of the cluster by oxidation. The purpose of these studies is to virtually screen ligands reported previously Boncella A.E. et al. [2], to obtain a library of compounds with given properties, which recommend them for binding proteins containing Fe-S clusters. To our knowledge, such a study, using hybrid DFT algorithms such as B3LYP, has not yet been performed. Previous encouraging results using quantum mechanical calculations, both on molecular and properties of interest for achieving the Quantitative Structure-Activity Relationship (QSAR) of

various natural or synthetic ligands for a deeper understanding of their structure, are reported [12-14]. These studies employing computational methods are crucial for evaluating ligands' suitability for pharmaceutical design, with a focus on bioavailability and biological activity, and foster new perspectives in this kind of approach, applicable to Fe-S ligand clusters. Such theoretical approaches include calculating properties and checking for adherence to specific rules for certain physicochemical properties, e.g., Lipinski's rule of five (ROF) [15] or Veber's criteria [16], to assess drug-likeness, specifically in terms of oral bioavailability and drug-like potential. Fe-S clusters, as redox centres by reversible electron transfer transitions, provide critical electron transfer for metabolic flux and genomic stability (e.g., oxidative phosphorylation, photosynthetic electron transport, DNA replication and repair), and other protective repair mechanisms (e.g. signalling and regulatory role under oxidative stress). They are considered to govern protein structure and functions in redox biology [17-20]. The redox potential is closely related and linearly dependent on the calculated energies of molecular frontier orbitals [13, 21], as previously shown for other compounds, indicating that computational approach is very useful and sufficiently accurate to estimate and tune the electrochemical redox behaviour.

2. DFT procedure

Firstly, the 3D structures of selected ligands from the literature survey [11] were optimized using energy minimization by means of corrected MMFF density functional model using Spartan'24 software (Win/64b) release 1.0.0 from Wavefunction, Inc. Irvine, CA, U.S.A. [22]. Secondly, setup of density functional algorithm and basis set was done (B3LYP/ 6-311 (d, p)) [23,24] at the equilibrium geometry; computations on molecular descriptors and properties have been performed using gas phase. The structures of the investigated ligands are depicted in the following figures, as monodentate (Fig. 2), bi-dentate (Fig. 3), and tri-dentate ligands (Fig. 4).

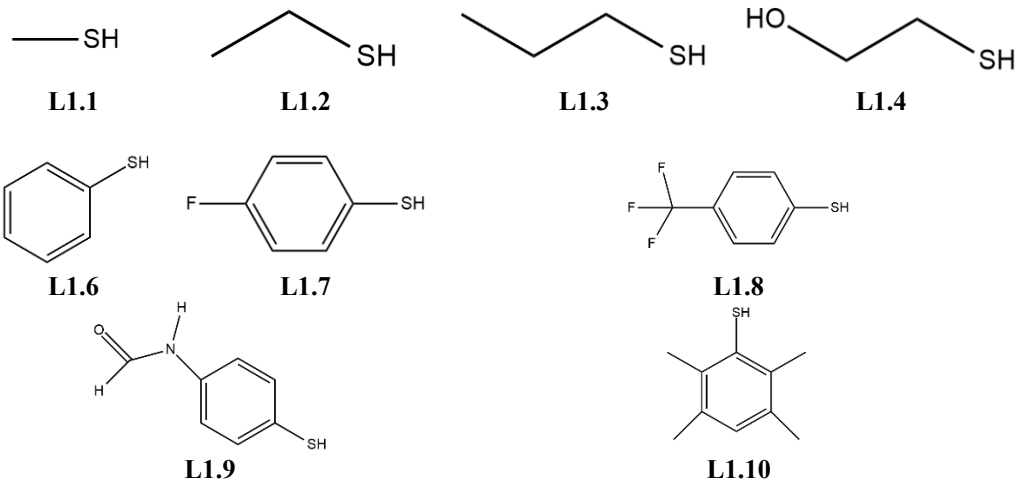

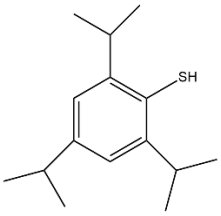

L1.11

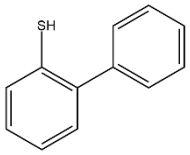

L1.12

Fig. 2. Structures of investigated monodentate ligands

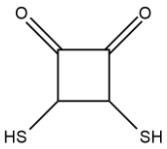

L2.2

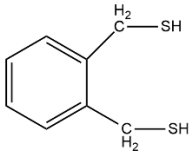

L2.3

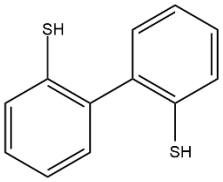

L2.4

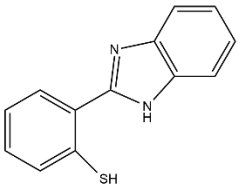

L2.5

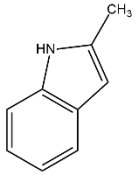

L2.6

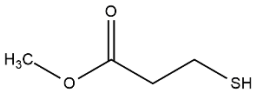

L2.7

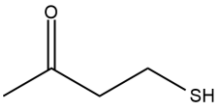

L2.8

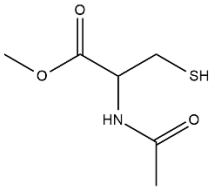

L2.9

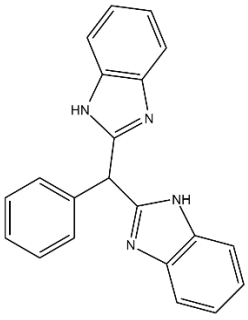

L2.10

Fig. 3. Structures of investigated bidentate ligands

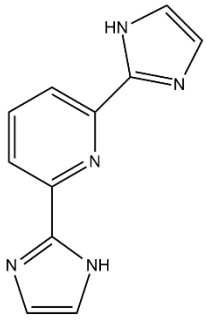

L3.0

Fig. 4. Structures of the investigated tridentate ligand

3. Results and Discussions

Table 1 lists the results of calculations referring to molecular properties (Table 1a) and QSAR properties (Table 1b) of monodentate ligands using B3LYP/6-311 (d, p) in vacuum, at equilibrium geometry. Similarly, for bi-dentate and tri-dentate ligands, respectively, the results are given in Table 2a, Table 2b, and Table 3a, Table 3b, respectively,

where: L – ligand, W – molar weight ($g \cdot mol^{-1}$), E - energy (a.u), D - dipole moment (Debye), Conf. - number of conformers, E_{HOMO} - energy of HOMO orbitals (eV), E_{LUMO} - energy of LUMO orbitals (eV); A – area ($Å^2$), V – volume ($Å^3$), PSA - polar surface area ($Å^2$), I.ov. - the ovality index, P - polarizability, logP - the water-octanol partition coefficient, HBD - the number of hydrogen bond donors, HBA - the number of hydrogen bond acceptors.

Table 1a

Molecular properties for monodentate ligands

Ligand/ Formula	W	E	D	Conf.	E_{HOMO}	E_{LUMO}
L1.1 / CH_4S	48.107	-438.733712	1.75	1	-6.62	0.17
L1.2 / C_2H_6S	62.134	-478.056863	1.83	3	-6.55	0.20
L1.3 / C_3H_8S	76.161	-517.380845	1.88	3	-6.54	0.21
L1.4 / C_2H_6O	78.134	-553.281885	1.06	27	-6.63	0.21
L1.5 / C_4H_9NOS	119.186	-686.106960	2.93	9	-6.68	-0.33
L1.6 / C_6H_6S	110.179	-630.508036	1.27	1	-6.14	-0.46
L1.7 / C_6H_5FS	128.169	-729.773587	0.96	1	-7.02	-0.85
L1.8 / $C_7H_5F_3S$	178.177	-967.499015	2.48	1	-6.63	-1.19
L1.9 / C_7H_7NOS	153.204	-799.244347	1.89	4	-6.58	-1.21
L1.10 / $C_{10}H_{14}S$	166.287	-787.801907	1.32	1	-5.98	-0.21
L1.11 / $C_{15}H_{24}S$	236.423	-984.403413	1.49	16	-6.37	-0.56
L1.12 / $C_{12}H_{10}S$	186.278	-861.6076	1.51	2	-6.03	-0.86

Table 1b

QSAR properties for monodentate ligands

Ligand / Formula	A	V	PSA	I.ov.	P	logP	HBD	HBA
L1.1 / CH_4S	72.78	51.01	0.00	1.09	43.91	0.56	1	1
L1.2 / C_2H_6S	93.25	69.53	0.00	1.14	45.42	0.89	1	1
L1.3 / C_3H_8S	112.80	87.85	0.00	1.18	46.91	1.21	1	1
L1.4 / C_2H_6O	102.67	76.96	20.076	1.17	46.00	0.04	2	2
L1.5 / C_4H_9NOS	149.06	122.02	14.971	1.25	49.77	-0.36	1	3
L1.6 / C_6H_6S	135.11	116.54	0.00	1.17	49.48	2.22	1	1
L1.7 / C_6H_5FS	141.56	121.35	0.00	1.19	49.76	2.38	1	1
L1.8 / $C_7H_5F_3S$	170.78	148.58	0.00	1.26	52.14	3.14	1	1
L1.9 / C_7H_7NOS	273.20	149.94	25.247	1.27	52.27	0.86	2	3
L1.10 / $C_{10}H_{14}S$	205.43	187.86	0.00	1.30	55.25	4.17	1	1
L1.11 / $C_{15}H_{24}S$	304.91	280.32	0.00	1.47	62.74	5.92	1	1
L1.12 / $C_{12}H_{10}S$	212.91	199.79	0.00	1.29	56.36	3.89	1	1

Table 2a

Molecular properties for bi-dentate ligands

Ligand/ Formula	W	E	D	Conf.	E_{HOMO}	E_{LUMO}
L2.2 / $C_4H_4O_2S_2$	148.203	-1101.72143	3.90	9	-7.00	-3.32
L2.3 / $C_8H_{10}S_2$	170.297	-1107.36343	2.94	36	-6.41	-0.95
L2.4 / $C_{12}H_{10}S_2$	218.341	-1259.81748	1.63	8	-6.19	-0.79
L2.5 / $C_{13}H_{10}N_2S$	226.302	-1009.26676	2.00	4	-6.00	-1.66
L2.6 / C_9H_9N	131.179	-403.223207	2.59	1	-5.51	-0.27
L2.7 / $C_4H_80_2S$	120.171	-705.990067	2.61	27	-6.70	-0.03
L2.8 / C_4H_8OS	104.172	-630.736221	3.00	27	-6.61	-0.77
L2.9 / $C_6H_{11}NO_3S$	177.223	-914.050723	4.80	162	-6.66	-0.51
L2.10 / $C_{21}H_{16}N_4$	324.388	-1029.13241	4.12	4	-5.96	-0.98

Table 2b

QSAR properties for bi-dentate ligands

Ligand / Formula	A	V	PSA	I.ov.	P	logP	HBD	HBA
L2.2 / $C_4H_4O_2S_2$	145.81	120.56	29.323	1.24	50.28	0.81	2	4
L2.3 / $C_8H_{10}S_2$	194.48	171.19	0.00	1.30	53.97	2.54	2	2
L2.4 / $C_{12}H_{10}S_2$	231.36	216.75	0.00	1.33	57.68	4.02	2	2
L2.5 / $C_{13}H_{10}N_2S$	240.09	226.14	17.189	1.34	58.69	4.53	1	2
L2.6 / C_9H_9N	167.80	150.34	11.983	1.23	52.33	2.16	1	1
L2.7 / $C_4H_80_2S$	147.46	117.93	20.704	1.27	49.36	0.38	1	2
L2.8 / C_4H_8OS	136.54	108.98	14.225	1.24	48.83	0.62	1	2
L2.9 / $C_6H_{11}NO_3S$	205.75	169.86	44.994	1.39	53.70	-0.73	2	4
L2.10 / $C_{21}H_{16}N_4$	348.43	336.77	36.722	1.49	67.51	6.69	0	2

Table 3a

Molecular properties for the tri-dentate ligand

Ligand/ Formula	W	E	D	Conf.	E_{HOMO}	E_{LUMO}
L3.0 / $C_{11}H_9N_5$	211.228	-698.504462	4.09	4	-5.84	-1.34

Table 3b

QSAR properties for the tri-dentate ligand

Ligand / Formula	A	V	PSA	I.ov.	P	logP	HBD	HBA
L3.0 / $C_{11}H_9N_5$	232.22	210.37	45.519	1.36	57.37	2.48	0	3

Interactions of ligands occurring in biological systems of aqueous and physiological media are strongly influenced by molecular features and descriptors of structures, that accurately can be evaluated employing computational approximations and visualized to depict the more susceptible area for hydrophobic/hydrophilic interactions or strong bonds (hydrogen bonding) within the interacting amino acids residues of the active binding site of given molecular targets, namely proteins/enzymes containing Fe-S clusters, in this case. Protomeric and tautomeric states of ligands, along with properties screened by pharmacological filters such as Lipinski [15] and Veber [16] including molecular weight (less than 500 Da), counts of hydrogen bonds acceptors and donors (HBD, and HBA respectively), the balance of hydrophilic/hydrophobic character given by the measure of the water-octanol partition coefficient (logP), the polar surface area and the sum of rotatable bonds are suggestive indications of druggability. In terms of HBD and HBA, all investigated structures have been found to meet the specified requirements imposed by Lipinski's rule, meaning less than 5 hydrogen bond donors and less than 10 hydrogen bond acceptors, proving good absorption and permeation in humans. In terms of molecular weight, all ligands have less than 500 Da; molecules under this threshold are more likely to be very well absorbed through membranes. Regarding the logP values, the most hydrophilic compound among monodentate ligands is L1.5 with logP = − 0.36, while L1.11 (logP = 5.92) is the most lipophilic (Table 1b). Among bidentate ligands, L1.5 is the most hydrophilic (logP = − 0.36), while L2.10 (logP = 6.69), the most lipophilic (Table 2b); L1.11 and L2.10 exceed the recommended value of logP, respectively 5. Concerning PSA values, given by the sum of heteroatoms' areas in the molecules, variations are noticed among the bidentate and tridentate ligands, but all values obey the limitation imposed by Veber and co-workers [16], which stated PSA < 140Å. logP and PSA are also important for the evaluation of the oral bioavailability [14], values of logP between 1.35 − 1.8 indicate good oral and intestinal absorption. None of the ligands are candidates for oral drugs, without structural improvement in order to overcome this limitation; L1.3 (2-propanethiol) reveals the closest value to this interval (logP = 1.21) and could be used further as a reference skeleton.

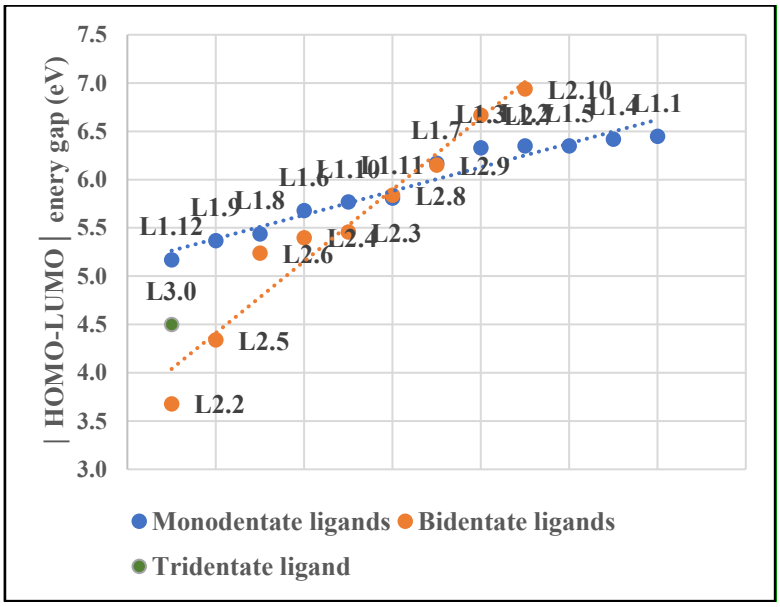

Fig. 5. Variation of the energy gap between HOMO and LUMO orbitals in the mono-, bi- and tridentate ligands.

An analysis of reactivity considering the difference in energy between the frontier molecular orbitals HOMO and LUMO, is shown in Fig. 5.

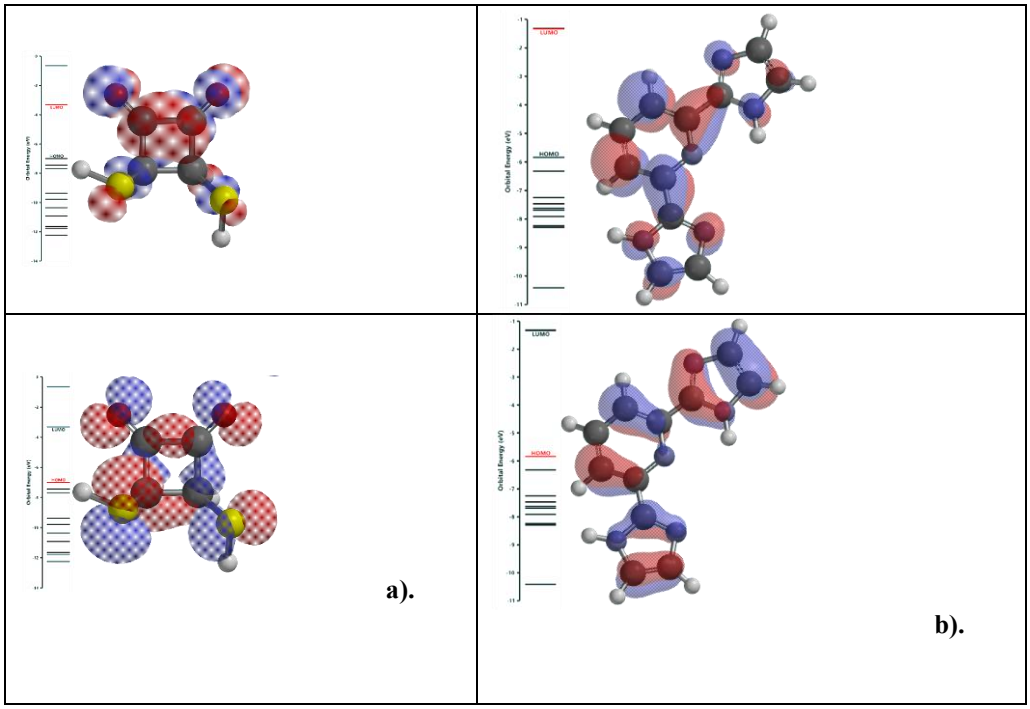

Fig. 6. HOMO – LUMO energy diagram for L2.2 (a) and L3.0 (b).

Larger energy gaps indicate less reactive molecules [25]. In the monodentate ligand series, L1.12 ligand shows the smallest energy gap (5.17 eV), suggesting the most reactive monodentate structure, and L1.1 reveals the largest energy gap (6.45 eV). Among bidentate ligands, L2.2 is the most reactive (energy gap = 3.68 eV), while L2.10 is the most stable (energy gap = 6.94 eV). The investigated tridentate ligand (L3.0) shows a moderate value of energy gap (4.5 eV). An example of HOMO – LUMO energy diagram is illustrated in Fig. 6, for L2.2 (Fig. 6a) and L3.0 (Fig. 6b) structures depicting the orbitals distribution over the skeleton structure and their energy levels in eV. As a result of the drug-likeness assessment by applying pharmacological filters for oral bioavailability, the key finding is that only the bidentate ligand L1.3 (2-propanethiol) can be used further as a lead compound for structure refinement for both oral and intestinal absorption. The limitation remains that the calculations are performed in the ground state, and future amendments related to the aqueous environment and pH are needed.

4. Conclusions

In this study, the density functional theory approach was helping to reveal structural attributes towards drug-likeness and biological activities of various ligands binding Fe-S cluster proteins, supporting their biological applications. Limitations are given by gas phase but are sufficient to evaluate in-depth structural descriptors important for the quantitative structure-activity relationships and further design of ligands able to make strong interactions leading to potential stable complexes with Fe-S clusters, which must be further demonstrated by molecular docking simulations.

Funding: This research was funded by the Ministry of Research, Innovation and Digitalization, Romania, through the “Nucleu” Program, Grant no. 1N/2023, PN 23-28 "BioChemLife", within the National Plan for Research and Development and Innovation 2022-2027, project no. PN 23-28 01 02.

Acknowledgments: All authors acknowledge support from COST Action, FeSImmChemNet. This article is based on work from COST Action FeSImmChemNet, CA21115, supported by COST (European Cooperation in Science and Technology).

R E F E R E N C E S

[1]. *Maio N., B.A.P. Lafont, D. Sil, Y. Li, J.M. Bollinger Jr, C. Krebs, Th. C. Pierson, W.M. Linehan, T.A. Rouault*, “Fe-S co-factors in the SARS-Cov-2 RNA-dependent RNA polymerase are potential antiviral targets”, in Science, **vol. 373**, 2021, pp. 236-241

[2]. *A.E. Boncella, E.T. Sabo, R.M. Santore, J. Carter, J. Whalen, J.D. Hudspeth, C.N. Morrisonx,* “Structure of XPD from Thermoplasma acidophilum, The expanding utility of iron-sulfur clusters: Their functional roles in biology, synthetic small molecules, maquettes and artificial proteins, biomimetic materials, and therapeutic strategies”, in Coord. Chem. Rev., **vol. 453**, 2022, pp. 214229

[3]. *S. Cosconati, J.A. Hong, E. Novellino, K.S. Carroll, D.S. Goodsell, A.J. Olson*, “Structure-based virtual screening and biological evaluation of Mycobacterium tuberculosis adenosine 5’-phosphosulfate reductase inhibitors”, in J. Med. Chem., **vol. 51**, 2008, pp. 6627-6630.

[4]. *L.A. Mike, B.F.; Dutter, J.L. Moorex, N.P. Vitko, O. Aranmolate, T.E. Kehi-Fie, S. Sullivan, P.R. Reidc, J.F. DuBois, A.R. Richardson, R.M. Capeioli, G.A. Sulikowski, E.P. Skaar,* “Activation of heme biosynthesis by a small molecule that is toxic to fermenting Staphyloccocus aureus”, in PNAS, **vol. 110**, 2013, 8206-8211

[5]. *J.E. Choby, L.A. Mike, A.A. Mashruwala, B.F. Dutter, P.M. Dunman, G.A. Sulikowski, J.M. Boyd, E.P. Skaar*, "A small-molecule inhibitor of iron-sulfur cluster assembly uncovers a link between virulence regulation and metabolism in Staphyloccocus aureus", in Cell. Chem. Biol., **vol. 23**, 2016, pp. 1351-1361

[6]. *B.F. Dutter, L.A. Mike, P.R. Reid*, "Decoupling activation of heme biosynthesis from anaerobic toxicity in a molecule active in Staphylococcus aureus", in ACS Chem. Biol., **vol. 11**, 2016, pp. 1354-1361

[7]. *P. Venkateswara Rao, R.H. Holm,* "Synthetic Analogues of the Active Sites of Iron−Sulfur Proteins", in Chem. Rev., **vol. 104**, no. 2, 2004, pp. 527–560

[8]. *J. Fitzpatrick, H. Kalyvas, M.R. Filipovic, I. Ivanović-Burmazović, J.C. MacDonald, J. Shearer, E. Kim,* "Transformation of a Mononitrosyl Iron Complex to a [2Fe-2S] Cluster by a Cysteine Analogue", in J. Am. Chem. Soc., **vol. 136**, no. 20, 2014, pp. 7229–7232

[9]. *J. Fitzpatrick, E. Kim,* "New Synthetic Routes to Iron–Sulfur Clusters: Deciphering the Repair Chemistry of [2Fe–2S] Clusters from Mononitrosyl Iron Complexes", in Inorg. Chem., **vol. 54**, no. 22, 2015, pp. 10559–10567

[10]. *J.S. Rieske, D.H. MacLennan, R. Coleman,* "Isolation and properties of an iron-protein from the (reduced coenzyme Q)-cytochrome C reductase complex of the respiratory chain. Biochem. Biophys. Res. Commun., **vol. 15**, 1964, pp. 338-344

[11]. *J. Ballmann, A. Albers, S. Demeshko, S. Dechert, E. Bill, E. Bothe, U. Ryde, F. Meyer,* "A synthetic analogue of Rieske-type [2Fe-2S] clusters", in Angew. Chem. Int. Ed. 2008, **vol. 47**, pp. 9537–9541

[12]. *A. Stefaniu, L.C. Pirvu,* "In Silico Study Approach on a Series of 50 Polyphenolic Compounds in Plants; A Comparison on the Bioavailability and Bioactivity Data", in Molecules, **vol. 27**, 2022, pp. 1413. https://doi.org/10.3390/molecules27041413

[13]. *O. Ciocirlan, E.-M. Ungureanu, A.-A. Vasile (Corbei), and A. Stefaniu,* "Properties Assessment by Quantum Mechanical Calculations for Azulenes Substituted with Thiophen– or Furan–Vinyl–Pyridine", in Symmetry, **vol. 14**, 2022, pp. 354. https://doi.org/10.3390/sym14020354

[14]. *A-A. Vasile (Corbei), A. Stefaniu, L. Pintilie, G. Stanciu, E.-M. Ungureanu,* "In silico characterization and preliminary anticancer assessment of some 1,3,4-thiadiazoles", in U.P.B. Sci. Bull., Series B, **vol. 83**, no. 3, 2021, pp. 3-12

[15]. *C.A. Lipinski, F. Lombardo, B.W. Dominy, P.J. Feeney,* "Experimental and computational approaches to estimate solubility and permeability in drug discovery and development settings", in Adv. Drug Deliv. Rev., **vol. 46**, 2001, pp. 3–26

[16]. *D.F. Veber, S.R. Johnson, H.Y. Cheng, B.R. Smith, K.W. Ward, K.D. Kopple,* "Molecular properties that influence the oral bioavailability of drug candidates", in J. Med. Chem., **vol. 45**, 2002, pp. 2615–2623

[17]. *J. Min, F. Ali, B.R. Brooks, B.D. Bruce, M. Amin,* "Predicting Iron−Sulfur Cluster Redox Potentials: A Simple Model.", in ACS Omega, **vol. 10**, iss.15, 2025, pp. 15790−15798

[18]. *M. Fontecave, B. Py, S. Ollagnier de Choudens, F. Barras,* "From iron and cysteine to iron-sulfur clusters: the biogenesis protein machineries", in EcoSal Plus **vol. 3**, iss. 1, 2008, 14

[19]. *J.C. Crack, P. Amara, E. de Rosny, C. Darnault, M.R. Stapleton, J. Green, A. Volbeda, J.C. Fontecilla-Camps, N.E. Le Brun,* "Probing the reactivity of [4Fe-4S] fumarate and nitrate (FNR) regulator with O_2 and NO: increased O_2 resistance and relative specificity for NO of the [4Fe-4S] L28H FNR cluster", in Inorganics, **vol. 11**, iss. 12, 2023, 450

[20]. *S. Jafari, Y.A. Santos, J. Bergmann, M. Irani, U. Ryde*, *Benchmark,* "Study of Redox Potential Calculations for Iron−Sulfur clusters in proteins", in Inorg. Chem. **vol. 61**, 2022, 5991-6007

[21]. *D.D. Méndez-Hernández, P. Tarakeshwar, D. Gust, T.A. Moore, A.L. Moore, V. Mujica,* "Simple and accurate correlation of experimental redox potentials and DFT-calculated HOMO/LUMO energies of polycyclic aromatic hydrocarbons", in J. Mol. Model., **vol. 19**, 2013, 2845–284

[22]. *Y. Shao, L.F. Molnar, Y. Jung, J. Kussmann, et al.,* "Advances in methods and algorithms in a modern quantum chemistry program package", in Phys. Chem. Chem. Phys., **vol. 8**, no. 27, 2006, pp. 3172-3191

[23]. *W.J. Hehre*, A Guide to Molecular Mechanics and Quantum Chemical Calculations, Wavefunction, Inc., Irvine, CA, 2003

[24]. *C. Lee, W. Yang, R.G. Parr,* "Development of the Colle-Salvetti Correlation-Energy Formula into a Functional of the Electron Density", in Phys. Rev. B, **vol. 37**, 1988, pp. 785–789

[25]. *P. Demir, F. Akman,* "Molecular structure, spectroscopic characterization, HOMO and LUMO analysis of PU and PCL grafted onto PEMA-co-PHEMA with DFT quantum chemical calculations", in J. Mol. Struct., **vol. 1134**, 2017, pp. 404–415.